energies

MDPI

Article

The Role of Emitters, Heat Pump Size, and Building Massive Envelope Elements on the Seasonal Energy Performance of Heat Pump-Based Heating Systems

Matteo Dongellini *, Paolo Valdiserri, Claudia Naldi and Gian Luca Morini

Department of Industrial Engineering, Alma Mater Studiorum—University of Bologna, Viale del Risorgimento 2, 40136 Bologna, Italy; paolo.valdiserri@unibo.it (P.V.); claudia.naldi2@unibo.it (C.N.); gianluca.morini3@unibo.it (G.L.M.)

* Correspondence: matteo.dongellini@unibo.it; Tel.: +39-051-209-0467

Received: 24 August 2020; Accepted: 28 September 2020; Published: 30 September 2020

Abstract: The influence of emitters, heat pump size and building envelope thermal inertia was investigated on the energy consumption of a heat pump-based heating system with a numerical study performed with the dynamic software TRNSYS. An algorithm based on a Thermal Inertia Control Logic (TICL), which can exploit the capability of the building envelope to store thermal energy, has been applied. When the proposed algorithm is employed, the indoor air temperature set-point is increased when the outdoor temperature is larger than the bivalent temperature of the building-heat pump system. Different configurations of the heating system were simulated considering either convective (fan-coil) or radiant (radiant floor) emitters coupled to a variable-speed air-to-water heat pump. Simulations have been carried out considering a reference building derived from the IEA SHC Task 44 and evaluating the influence of the proposed control logic on both the heat pump seasonal energy performance and the internal comfort conditions perceived by the building users. The obtained results highlight how the introduced TICL can guarantee the use of downsized heat pumps, coupled to radiant emitters, with a significant enhancement of the seasonal performance factor up to 10% and a slight improvement of comfort conditions. On the other hand, when convective terminal units are considered the proposed logic is not effective and the overall energy consumption of the system increases up to 15%.

Keywords: air-to-water heat pumps; envelope thermal inertia; demand response logic; thermal comfort; seasonal energy performance

1. Introduction

Presently, in many countries, buildings are liable to a significant share of the overall energy demand: in the European Union (EU) the building sector accounts for about 36% of greenhouse gases emissions and about 40% of the European final energy consumption [1–3]; in Italy the energy consumption for civil use has been assessed at 48 Mtep, around 37% of the total energy consumed [4]. Moreover, if the analysis is restricted to the Public Administration building stock, the electric and thermal consumptions cover the 8% and 10% of national demand, respectively [5].

The reduction of building energy needs and, consequently, the limitation of global warming plays a crucial role in energy saving in all the countries. Space heating energy demand is mainly linked to energy losses through the building envelope: transparent components account for 23% of the energy consumption, while among opaque elements the highest share is related to external walls (25%) and roofs (22%) [6]. Those data point out that in order to significantly reduce energy use a huge potential is related to the improvement of building envelope components. In fact, many studies have been

performed on envelope design strategies for various types of buildings [7]: public or private, new constructions and in the retrofitting of existing stock located in different cities with distinct climates [8,9]. A critical aspect is represented by windows but, with a proper transparent components design, the adoption of glasses large openings can translate into significant energy savings and occupant comfort improvement [10,11].

To promote the decarbonization of building stock in Europe, it is recently published the Directive 2018/844 on the Energy Performance of Buildings [12]; among other relevant topics, the Directive highlights the importance of assuring smart buildings with the capability to adapt the building energy demand to the effective user needs. Moreover, the grid requirements and the ambient conditions, as well as the improvement between building energy needs and the energy distribution infrastructure should be guaranteed [13]. One simple and promising demand response application is the use of thermal capacitance of envelope components and thermal energy storage to shift the building's thermal load and, consequently, the absorbed load of electrical HVAC devices, such as heat pumps and air conditioners. More in detail, all buildings are able to store thermal energy in their envelope, thanks to the presence of massive elements (i.e., outer walls, roofs, ceilings): this available amount of stored energy can be used to passively optimize the performance of HVAC systems [14,15]. In many Near Zero-Energy Building (NZEB) solutions, the increase of thermal capacitance of envelope components is used as an effective solution to enhance the energy performance of the building: phase change materials (PCMs) have been tested as a suitable technology due to their high storing capability per unit of volume [6,16]. Nonetheless, PCMs are still characterized by a series of drawbacks, such as the flammability risk, the limited stability in time and the significant cost [17], which limits their applications and diffusion on the market.

Playing on the characteristics of the envelope thermal capacity, it is possible to delay the activation of HVAC systems without worsening indoor thermal comfort conditions. In fact, if building thermal zones are pre-heated (pre-cooled) before the shutdown of space heating (cooling) operating mode, by using the heat stored in the envelope massive elements it is possible to stabilize the indoor thermal conditions by delaying the re-activation of the HVAC system. To increase the heat stored in the envelope elements, the indoor air set-point temperature can be increased (decreased) in correspondence of favorable external conditions. However, it is important to stress that the internal operative temperature has to be maintained within a defined range to guarantee proper comfort. Moreover, it has been demonstrated that the typology of HVAC emitters has a strong impact on the capability of re-charging the massive envelope elements with thermal energy [18]. Convective heat emitters, such as fan-coils and high-temperature radiators, are able to interact directly with indoor air and, for this reason, their effect on the re-charge of the massive envelope elements is limited. On the contrary, radiant terminal units such as ceiling or under-floor radiant surfaces are able to thermally activate the envelope components with a reduced direct effect on the internal air temperature.

Presently, electric-driven heat pumps (HPs) represent the most promising technology to fulfill the strict requirements linked to the exploitation of renewable energy sources [19,20]: heat pumps can satisfy all the energy end-uses of buildings through a single device and could guarantee significant energy savings if compared to traditional HVAC systems [21]. Furthermore, heat pumps can be easily coupled to demand response programs based on the accumulation of heat within the building envelope: according to this kind of control logics, the heat pump operation could be flexibly determined on the basis of electric market conditions (i.e., electric energy cost) and outdoor conditions. The analysis of literature points out that several authors focused their research on demand response programs applied to heat pumps [22,23] in order to shave the absorbed peak power by means of specific control algorithms, which allow partially decoupling thermal and electrical loads.

Conversely, in the present paper, we propose a different strategy: the heat storage capacity of the building envelope has been used to enhance both the seasonal energy performance of heating systems based on air-to-water heat pumps and indoor comfort conditions. Despite of the papers previously published in the literature, this work wants to investigate the effects of a demand response control

logic which affects the internal conditions and allows directly storing thermal energy within all the building envelope components. Moreover, in this paper the performance of the proposed algorithm has been evaluated taking into account the typology of terminal units: convective and radiant emitters have been considered and the seasonal performance of the whole heating system has been evaluated through of a series of numerical dynamic simulations.

According to the proposed algorithm, when the external air temperature is higher than the bivalent temperature (i.e., the external air temperature in correspondence of which the heat pump heating capacity equals the building thermal load), the indoor air temperature set-point is increased, with the aim to store thermal energy in the massive envelope elements when the heat pump heating capacity exceeds the building required load. When the external temperature is lower than the bivalent temperature, the excess of heat stored in the envelope can be used as a passive backup of the heat pump, avoiding the activation of electrical resistances or alternative active backup systems. Different configurations of the heating system have been considered in the presented simulations by varying the heat pump size in combination with fan-coils or under-floor radiant heating surfaces in order to evaluate the influence of the emitters on the effectiveness of the proposed algorithm.

2. Methodology

A numerical model of a heat pump-based heating system coupled to a residential building has been made by means of TRNSYS 17 [24]. The TRNSYS dynamic model allows taking into account the performance of all the elements of the heating system such as the variable-speed air-to-water heat pump, the emitters, the hydronic distribution loop and the control system. The building thermal loads are calculated by means of TRNSYS Type 56 (Multi-zone building, [25]). In Figure 1 the TRNSYS model developed in this work for both emitters typology is shown for reference.

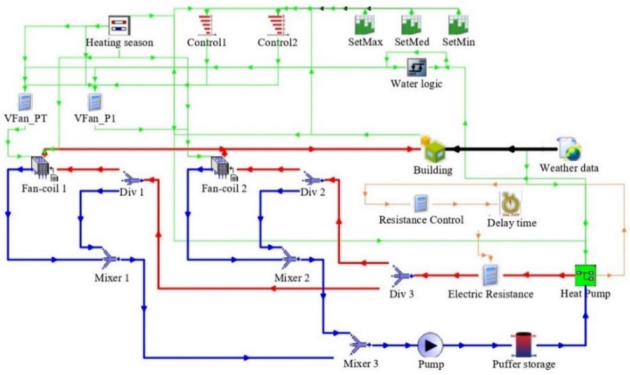

(**a**)

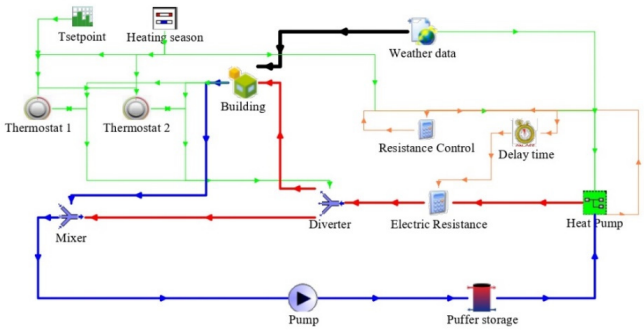

(**b**)

Figure 1. Layout of the heat pump heating systems developed by means of TRNSYS 17 environment: (**a**) based on fan-coils; (**b**) based on under-floor radiant heating.

2.1. Building Modeling and Climatic Data

The building considered for simulations is derived from the IEA SHC Task 44 [26], where three different buildings (SFH15, SFH45, SFH100), characterized by the same geometry and variable envelope thermal insulation, are defined. In this paper, the SFH45 building has been considered for reference; in Figure 2 a tri-dimensional view of the building is shown, while in Table 1 the main characteristics of the envelope elements are reported.

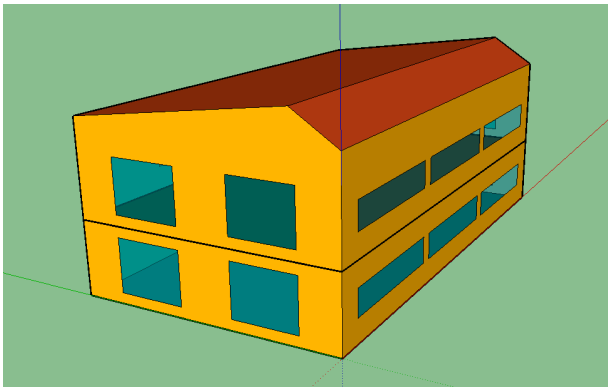

Figure 2. Tri-dimensional view of the residential building considered in the present paper.

Table 1. Geometrical and thermo-physical data of the building envelope components.

Assembly	Thickness (m)	U-Value (W m^{-2} K^{-1})
External wall	0.318	0.364
Ground floor	0.385	0.241
Floor	0.185	0.235
Roof	0.285	0.694
Internal wall	0.200	0.885
Total floor area (m^2)	360	
Net heated volume (m^3)	1251	

This study was carried out by considering the building placed in Milan (North of Italy, 45°28′ North, 9°10′ East): in this location, the degree days are 2404, while the design and average outdoor air temperature are equal to −5 °C and 11.7 °C, respectively.

The simulation covers the whole conventional heating season for Milan (i.e., from 15 October to 15 April, corresponding to 183 days). The heating design load has been calculated with an indoor set-point temperature of 22 °C (when fan-coils are considered to be emitters) and it is equal to 8.3 kW in correspondence of the design outdoor air temperature (−5 °C). On the other hand, an indoor set-point temperature of 20.5 °C is considered in presence of underfloor radiant heating surfaces. Different set-point values for the internal air have been defined depending on the heat emitter typology in order to guarantee the same indoor comfort conditions and make the results obtained for the two simulated configurations comparable one another. The selected set-point temperatures are chosen within the range indicated by the European standard EN 7730 [27] for the comfort class B.

2.2. Characterization of the Heating System

The heating system coupled to the reference building described in the previous section is based on an inverter-driven air-to-water heat pump. To investigate the different behavior of the heating system when the heat pump is coupled to convective or radiant heat emitters, two different models have been developed: in the first one (Case A, shown in Figure 1a) space heating is provided by two-pipe three-speed fan-coils, while in the second configuration (Case B, reported in Figure 1b) thermal zones

are heated by means of under-floor radiant heating surfaces. Depending on the emitters, the supply water temperature of the heating system has been fixed equal to 45 °C and 35 °C for cases A and B, respectively.

On the other hand, both the emitters have been sized with a nominal temperature difference between supply and return line equal to 5 °C. In Table 2 the main technical data of both fan-coil units and radiant floor heating are summarized: these data have been obtained from the manufacturer technical datasheets. $V_{w,RF}$ and $V_{w,FC}$ are the water volumetric flow rate of radiant floor heating and fan-coil respectively, V_{air} is the air volumetric flow rate, $P_{h,FC}$ is the fan-coil heating capacity and $P_{el,fan}$ is the electric power absorbed by the fan. It is important to highlight that fan-coil performance data are reported for the maximum, medium, and minimum speed of the fan evaluated with an indoor air temperature of 20 °C and with an inlet/outlet water temperature of 45/40 °C. The radiant floor rated heating capacity reported in Table 2 is calculated following the procedure suggested by the European standard EN 1264 [28], for inlet and outlet water temperature equal to 35 °C and 30 °C, respectively.

Table 2. Main technical data of emitters.

	Ground Floor				First Floor			
Fan-Coils	V_{air} ($m^3\ h^{-1}$)	$P_{h,FC}$ (W)	$P_{el,fan}$ (W)	$V_{w,FC}$ ($m^3\ h^{-1}$)	V_{air} ($m^3\ h^{-1}$)	$P_{h,FC}$ (W)	$P_{el,fan}$ (W)	$V_{w,FC}$ ($m^3\ h^{-1}$)
Minimum	320	2210	40		470	3530	47	
Medium	450	2910	50	0.655	605	4370	68	0.937
Maximum	640	3770	65		785	5390	98	
	Ground Floor				**First Floor**			
Under-Floor Radiant Surfaces	**Nominal Heating Capacity (W m^{-2})**	**Pipe Spacing (m)**		$V_{w,RF}$ ($m^3\ h^{-1}$)	**Nominal Heating Capacity (W m^{-2})**	**Pipe Spacing (m)**		$V_{w,RF}$ ($m^3\ h^{-1}$)
	20.6	0.30		0.850	29.3	0.20		1.137

The heating system is based on a variable-speed air-to-water heat pump. Three heat pumps, characterized by different sizes, have been considered to be heat generators. All the modeled heat pump units use R410A as refrigerant fluid and are produced by the same manufacturer. The biggest model (Unit 1) has a reference heating capacity at full load equal to 10.5 kW (in correspondence of an external air temperature of 7 °C, and with an inlet/outlet water temperature of 40/45 °C). Unit 1 results slightly oversized for the building design load while the smaller Unit 2 and Unit 3 are characterized by a reference heating capacity equal to 6.80 and 5.46 kW, respectively, in correspondence of the same reference conditions considered for Unit 1. In Figure 3 the performance data (i.e., heating capacity and Coefficient Of Performance (COP)) of the modeled heat pumps are reported as a function of the outdoor air temperature and of the inverter frequency φ (maximum frequency φ_{max}, minimum frequency φ_{min} and two intermediate frequencies φ_1 and φ_2), by fixing the inlet/outlet water temperature equal to 40/45 °C.

It is important to highlight that the performance data reported in Figure 3 have been obtained from the manufacturer and have been validated by means of experimental measures carried out in the manufacturer's test room. As pointed out by Figure 3b,d,f, all the considered units are characterized by higher values of COP at partial load: in fact, when the inverter frequency and, as a consequence, the compressor rotating speed decreases, the refrigerant flow rate decreases as well and the effective heat transfer area within heat exchangers increases, thus enhancing the unit efficiency.

Figure 4 shows both the heat pumps heating capacity at full load and the building thermal load, calculated by means of TRNSYS, as a function of the outdoor air temperature: by observing Figure 4 it is evident that Unit 1 satisfies the building heating load during the whole season without the need for a backup system. In fact, Unit 1 coupled to the reference building is characterized by a bivalent temperature T_{biv} close to the design outdoor temperature of Milan (−5 °C). When the outdoor temperature is higher than T_{biv}, the heating capacity supplied to the building must be modulated and the inverter frequency decreases; as pointed out by Figure 3a, Unit 1 is able to reduce its heating capacity up to 20% of the full load value and, for this reason, the building energy demand is perfectly matched for a large part of the season when this unit is adopted as a heat generator.

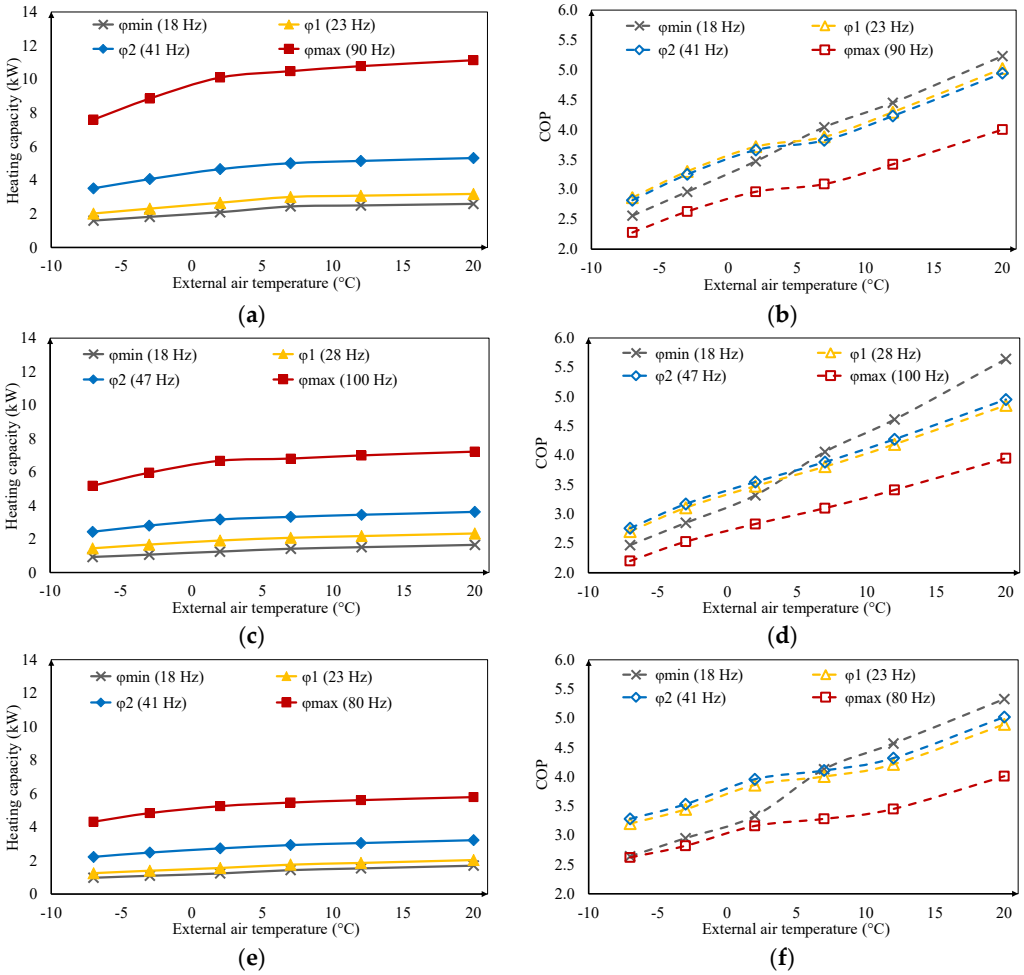

Figure 3. Performance data of the modeled variable-speed air-to-water heat pumps: (**a**) Heating capacity and (**b**) COP of Unit 1; (**c**) Heating capacity and (**d**) COP of Unit 2; (**e**) Heating capacity and (**f**) COP of Unit 3.

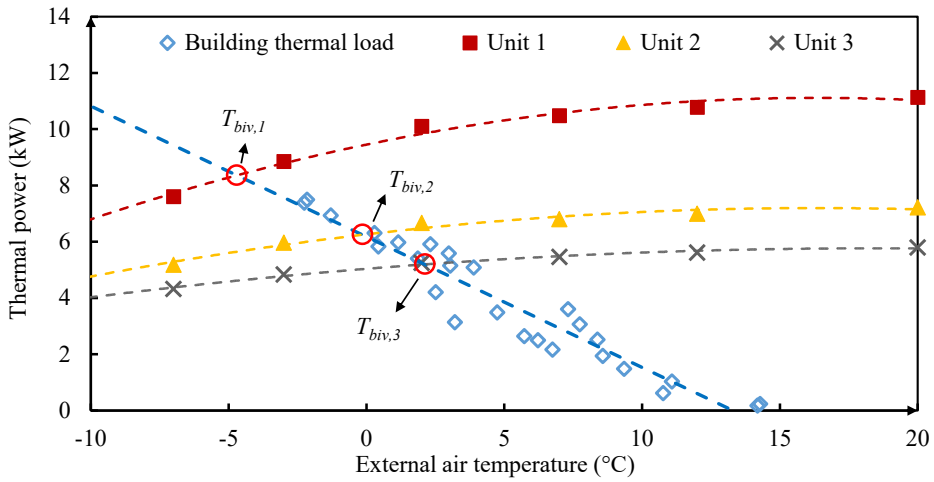

Figure 4. Building thermal load and heat pump heating capacity at full load as a function of external air temperature.

On the other hand, smaller heat pumps (i.e., Unit 2 and 3) are downsized concerning the effective energy need: Figure 4 shows that the bivalent temperature is equal to 0 °C and 2 °C for Unit 2 and

Unit 3, respectively. In these cases, when the external temperature is lower than T_{biv}, the heat pump operates at full load and a backup generator must be activated in order to cover the building energy need. The backup heat generator considered in this paper is an electric resistance (ER) characterized by a heating capacity of 2 kW. The back-up heater size has been selected according to the typical values of the back-up electrical resistances coupled to commercial heat pumps (up to three resistances with a heating capacity of 2 kW each).

2.3. Heating Control System

Typically, the control algorithm of inverter-driven heat pumps uses the supply water temperature $T_{w,out}$ (whose set-point value is equal to 45 °C for fan-coils and 35 °C for under-floor radiant heating surfaces) as monitored variable to control the thermal power of the device, evaluate the effective inverter frequency and modulate the heat pump heating capacity. For this reason, a Proportional-Integral-Derivative (PID) controller has been introduced in the dynamic model of the system to calculate the effective inverter frequency for each simulation timestep. Furthermore, when the minimum inverter frequency (φ_{min}) is reached and no further modulation is possible, an additional on-off algorithm is used by the heat pump to match the building thermal load: this logic is based on a hysteresis cycle, characterized by a 5 °C band centered on the set-point value defined by the PID controller for the supply water temperature. PID parameters (i.e., proportional gain K_p, integral time T_i and derivative time T_d) have been set according to heat pump manufacturer typical values: commercial units adopt a pure PI control logic and, for this reason, K_p, T_i and T_d have been fixed equal to 10 s, 300 s and 0 s respectively, regardless the adopted heat emitter.

The control of the backup electric resistance is based on the supply water temperature as well and, moreover, it adopts a time-temperature logic. More in detail, when the temperature of the supply hot water is lower than the set-point value for a fixed time period, the electric resistance is switched on. The delay time is needed in order to prevent unnecessary activations of the electric resistance and its value depends on the typology of emitters coupled to the heat pump: this delay is shorter for terminal units characterized by low thermal inertia (convective emitters such as fan-coils) and longer for high inertia devices (radiant emitters). In this work, the delay time has been fixed equal to 45 and 90 min for fan-coils and under-floor heating, respectively. Both these values have been defined according to the manufacturer control algorithms of commercial units.

Regarding the terminal units, their management is based on the indoor air temperature. When fan-coils are considered to be heat emitters, the fan speed is selected by the device on-board controller among the three possible values (i.e., minimum, medium and maximum speed) on the basis of a three-stage on-off controller, characterized by a different hysteresis dead band for each stage. In this case, the set-point value for indoor air temperature is equal to 22 °C. On the other hand, when the building is heated by means of radiant floor surfaces, the internal air set-point temperature has been fixed to 20.5 °C and an on-off thermostat characterized by a 1 °C dead band is used to manage the under-floor heating operation.

Moreover, the night set-back, typical for residential applications, has been introduced in the model: the above-mentioned set-point values of the indoor temperature are imposed each day from 7:00 to 23:00, while during night hours the set-point temperature has been fixed to 16 °C for both configurations.

In addition to the control logics previously described, a demand response control algorithm able to exploit the thermal inertia of the building envelope has been implemented in order to store thermal energy within massive envelope components. With the proposed logic, referred to as Thermal Inertia Control Logic (TICL), the heating system stores thermal energy in the massive elements of the envelope when the outdoor air temperature is larger than the system bivalent temperature. To charge the building of thermal energy, the set-point of the indoor air temperature is increased of 2 °C for each configuration. In particular, the indoor air temperature set-point is increased to 24 °C in presence of fan-coils (Case C) and to 22.5 °C in presence of radiant floor surfaces (Case D), respectively, when the ambient temperature is higher than −5 °C (Unit 1), 0 °C (Unit 2) and 2 °C (Unit 3). According to the

demand response logic TICL introduced in this paper, it is possible to postpone the modulation of the heat pump by increasing the hours during which the heat pump works at full load by enhancing both the seasonal energy performance of the heating system and the indoor thermal comfort conditions.

3. Results and Discussion

The numerical results presented in this section have been carried out considering the reference building SFH45 derived from the IEA SHC Task 44. Studies and simulations based on reference buildings are convenient to compare and allow scientists and engineers to relate results derived from different analyses.

Yearly dynamic simulations have been performed by considering a simulation time step equal to 30 s by covering the whole standard heating season of Milan, in order to compare the seasonal energy performance of the simulated configurations. According to the European standard EN 14825 [29], the seasonal efficiency of a heat pump system can be evaluated by means of two key performance indicators: the net Seasonal Coefficient of Performance ($SCOP_{net}$) and the Seasonal Coefficient of Performance of the whole system (SCOP), respectively defined as:

$$SCOP_{net} = \frac{E_{th,HP}}{E_{el,HP}} \quad (1)$$

$$SCOP = \frac{E_{th,HP} + E_{th,ER}}{E_{el,HP} + E_{el,ER}} \quad (2)$$

where $E_{th,HP}$ and $E_{th,ER}$ are the thermal energy supplied by the heat pump and the electric resistance during the heating season, respectively, while $E_{el,HP}$ and $E_{el,ER}$ are the electrical energy consumptions of the heat pump and the back-up heater during the heating season, respectively. Furthermore, in the following part of the paper, the overall thermal energy supplied to the building and the total electric energy consumption of the heating system are indicated as $E_{th,tot}$ and $E_{el,tot}$, respectively. For the sake of simplicity, an efficiency equal to 1 has been assumed for the electric resistance along the whole season: for this reason, $E_{el.ER}$ and $E_{th,ER}$ are equal for each timestep and, thus, also on a seasonal basis.

Indoor thermal comfort conditions must be guaranteed for building users during the whole season: the methodology reported by the European standard EN ISO 7730 has been used to assess internal thermal comfort. The Predicted Mean Vote (PMV) has been considered to be reference indicator to estimate comfort conditions and its value has been evaluated as a function of internal air temperature, mean radiant temperature and indoor relative humidity, calculated with TRNSYS, by fixing internal air velocity, occupants metabolic rate and clothing factor equal to 0.1 m/s, 1.2 met (sedentary activity) and 1 clo (typical winter clothing), respectively. Moreover, in Table 3 the discomfort period is shown for both configurations: this period highlights the number of hours in correspondence of which the PMV goes beyond the recommended limits for comfort (i.e., PMV lower than −0.5 or higher than +0.5, corresponding to thermal comfort class B for standard EN ISO 7730).

In Table 3, the seasonal energy consumption values of the simulated systems are reported by considering separately Case A (fan-coils as emitters) and Case B (radiant floor). The consumption data shown in Table 3 have been obtained without the introduction of the demand response logic described in the previous section (Section 2.3). It is important to emphasize that the reported PMV values have been calculated as the average along the heating period, not taking into account night hours with an imposed set-back on the internal set-point temperature.

Results show that with conventional control of the heating system, without the exploitation of the building thermal inertia, the heat pump sized on the building peak load (i.e., Unit 1) represents the most efficient solution in presence of both the emitters. In fact, when the generator size is reduced, the heat pump performance $SCOP_{net}$ increases up to 13% and 7% for fan-coils and radiant floor heating, respectively, but, on the other hand, the energy consumption linked to the backup system (i.e., electric heater) strongly increases as well. As a consequence, the energy performance of the whole system

(SCOP) significantly decreases by scaling from Unit 1 to Unit 3: SCOP is reduced by about 21% for Case A and about 25% for Case B.

Besides, Case B is characterized by SCOP values greater than those obtained for Case A and this is mainly due to the reduced supply temperature needed by radiant floors with respect to fan-coils. However, the increase of SCOP moving from Case B to Case A ranges between +5% and −1%, as pointed out by Table 3. This modest increase of SCOP is due to the large thermal inertia of conventional radiant floors: in presence of radiant floors, during the unsteady phases due to the re-activation of the heating system, the heat pump operates with higher frequency values with respect to Case A. As pointed out by Figure 3, COP is lower at the maximum inverter frequency and, for this reason, the overall energy performance of the system is enhanced when the heat pump is coupled to low-inertia emitters (Case A).

Table 3. Seasonal energy consumptions and key performance indicators of the simulated systems without TICL.

	Case A (Fan-Coil)			Case B (Radiant Floor)		
	Unit 1	**Unit 2**	**Unit 3**	**Unit 1**	**Unit 2**	**Unit 3**
$E_{th,HP}$ (kWh)	15,373	12,979	11,937	16,243	13,397	11,870
$E_{el,HP}$ (kWh)	5407	4288	3718	5415	4233	3690
$E_{th,ER}$ (kWh)	58	2223	2929	149	2403	3025
$E_{el,ER}$ (kWh)	58	2223	2929	149	2403	3025
$E_{th,tot}$ (kWh)	15,431	15,202	14,866	16,392	15,800	14,895
$E_{el,tot}$ (kWh)	5465	6511	6647	5564	6636	6715
$SCOP_{net}$	2.84	3.03	3.21	3.00	3.16	3.22
SCOP	2.82	2.33	2.24	2.95	2.38	2.22
PMV	−0.26	−0.28	−0.34	−0.12	−0.19	−0.25
Discomfort time (number of hours)	503	542	624	225	378	497

On the other hand, the values of PMV reported in Table 3 highlight that the emitter typology influences the thermal indoor comfort perceived by the users: by considering Case A, indoor comfort conditions are included within the comfort class B according to the standard EN ISO 7730 (i.e., average PMV between −0.5 and +0.5), while for Case B better comfort conditions are achieved by selecting Unit 1 and Unit 2, with a seasonal value of PMV corresponding to comfort class A (i.e., predicted mean vote between −0.2 and +0.2). This is due to the fact that radiant floors are able to increase significantly the average radiant temperature of the thermal zone by guaranteeing higher values of the operative temperature and better comfort conditions. These results are strengthened by the duration of discomfort periods reported in Table 3: the discomfort time is significantly higher for convective terminal units if compared to radiative emitters. For example, when Unit 3 is selected in configuration A, almost 20% of the heating period is characterized by thermal discomfort conditions.

The numerical simulations have been repeated by introducing the demand response control logic (TICL) in order to exploit the thermal inertia of the building more significantly. As mentioned before, the new control strategy introduced in this paper leads to the increase of the indoor air temperature set-point in presence of outdoor air temperature values larger than the bivalent temperature of the system.

As shown in Table 4, the proposed control strategy influences the behavior of the heating system. First of all, the overall thermal energy supplied to the building ($E_{th,tot}$) increases in presence of both the emitters. When fan-coils are considered to be terminal units (Case C), this increment is independent from the heat pump sizing and is almost equal to +16% (+8% per 1 °C of increase of the indoor air setpoint). On the contrary, in the presence of radiant heating surfaces (Case D) $E_{th,tot}$ rises from +31% to +10% by scaling from Unit 1 to Unit 3.

Table 4. Seasonal energy consumptions and key performance indicators of the simulated systems with the adoption of TICL algorithm.

	Case C (Fan-Coil + TICL)			Case D (Radiant Floor + TICL)		
	Unit 1	**Unit 2**	**Unit 3**	**Unit 1**	**Unit 2**	**Unit 3**
$E_{th,HP}$ (kWh)	17,866	15,142	13,865	21,172	16,389	13,845
$E_{el,HP}$ (kWh)	6152	4933	4289	6874	5042	4214
$E_{th,ER}$ (kWh)	137	2423	3361	284	1893	2489
$E_{el,ER}$ (kWh)	137	2423	3361	284	1893	2489
$E_{th,tot}$ (kWh)	18,003	17,565	17,226	21,456	18,282	16,334
$E_{el,tot}$ (kWh)	6289	7356	7650	7158	6935	6703
$SCOP_{net}$	2.90	3.07	3.23	3.08	3.25	3.29
SCOP	2.86	2.39	2.25	3.00	2.64	2.44
PMV	0.22	0.16	0.12	0.52	0.18	−0.14
Discomfort time (number of hours)	238	287	408	2349	306	283

As a consequence of the indoor air temperature increment, also PMV values increase when the TICL algorithm is introduced: average indoor conditions are in comfort class A for all simulated configurations except for Case D with Unit 1. In this case, in fact, the building is overheated by the HVAC system because, in presence of a control logic able to exploit the thermal energy stored in the building, Unit 1 becomes oversized: more than 2300 h of the heating period are linked to discomfort conditions, due to excessive internal temperatures. Furthermore, results point out that the overall energy consumption of this configuration (Case D—Unit 1) increases of about 28% for the configuration (Case B—Unit 1), with more frequent use of the electric resistance.

Conversely, the adoption of the TICL allows increasing the seasonal energy performance of the Cases based on undersized heat pumps (i.e., Unit 2 and 3). In these cases, an increase of SCOP of about +10% is observed for Case D with respect to Case B. By comparing Tables 3 and 4, it is evident that the backup energy consumption linked to the electric resistance decreases and, simultaneously, the electric energy absorbed by the heat pump increases. Results point out that with the adoption of the proposed demand response strategy, the heat pump is able to operate for a longer period during the milder part of the day at full load and the thermal energy surplus delivered to the building is stored in the envelope massive elements. Then, during the colder part of the day, the building envelope components release the accumulated energy and the electric heater activation is avoided or delayed. Nevertheless, the effectiveness of the proposed demand response algorithm is reduced by the behavior of the considered heat pumps at partial load: as pointed out by performance data reported in Figure 3, the simulated units poorly perform at full load with respect to part-load conditions. Since the heat pumps operate for a longer period at the maximum inverter frequency, their energy performance is unavoidably penalized. On the other hand, by comparing the values of $SCOP_{net}$ shown in Tables 3 and 4 it is evident that according to the proposed TICL algorithm, the heat pump seasonal energy performance slightly increases for all cases: in fact, the heat generator operates in correspondence of favorable ambient conditions (i.e., higher external air temperature) for a longer duration.

In addition, with this management strategy, the indoor thermal comfort is slightly improved: when the smallest heat pump is considered (i.e., Unit 3) in combination with a radiant floor, the average indoor conditions are able to vary from comfort class B (Case B—Unit 3) to comfort class A (Case D—Unit 3). Moreover, the period characterized by discomfort conditions is strongly reduced: the discomfort time decreases by 19% and 43% for Units 2 and 3, respectively.

Finally, results reported in Table 4 highlight that if convective emitters (fan-coils) are considered, no significant benefits can be achieved by adopting a control logic able to exploit the building thermal inertia. By comparing the results obtained for Case A with those of Case C it is evident that the seasonal electric energy consumption increases of about 15% for both heat pump and electric resistance. Nonetheless, also in these cases, indoor comfort conditions are improved, mainly due to the increase of the indoor air temperature set-point.

Present data indicate that the thermal inertia of the massive elements of a building envelope can be exploited in an efficient way only when radiant terminal units are adopted. In conclusion, in the presence of an undersized heat pump coupled to radiant emitters, an increase of the indoor air temperature set-point when the outdoor temperature is larger than the bivalent temperature of the system allows accumulating thermal energy in the building envelope elements. The accumulated thermal energy can be used as backup energy when the outdoor temperature becomes lower than the bivalent temperature by improving the average indoor comfort conditions and reducing the intervention of the electric resistance during the heating season.

4. Conclusions

In this paper, an innovative demand response control logic (TICL) for heat pump-based heating systems has been defined and tested by means of a series of yearly energy dynamic simulations. The proposed TICL heat pump control strategy allows accumulating thermal energy within the massive elements of the building envelope when the outdoor air temperature is larger than the bivalent temperature of the system, exploiting the thermal energy stored in the building during the coldest winter hours. The dynamic model of a residential building located in Milan (Italy) and coupled to a bivalent heating system composed by an air-to-water heat pump and a back-up electric resistance has been implemented by using TRNSYS; a series of yearly simulations has been carried out in order to evaluate the influence of the emitters' typology (convective or radiative) on the effectiveness of the TICL strategy along the whole heating season. Two configurations of the heating system have been considered: in the first one, two-pipe three-speed fan-coils are coupled to the heat pump while in the second one radiant floor surfaces are employed. For each configuration three heat pumps of different size have been simulated: Unit 1 is sized to match the building peak load, while Unit 2 and Unit 3 give a bivalent temperature larger than the design external air temperature of Milan (−5 °C) and, for this reason, the integration of the electrical back-up heater is needed. The TICL algorithm defined in this paper allows storing thermal energy within the massive elements of the building envelope in correspondence of favorable external conditions, by increasing the indoor air temperature set-point of 2 °C.

Adopting the TICL, it is possible to guarantee significant improvements only if radiant emitters are coupled to the heat pump. The numerical results demonstrate that the introduction of the proposed algorithm can increase up to +10% the seasonal energy performance of heating systems based on undersized heat pumps by exploiting the thermal inertia of the massive elements of the building. The overall electrical energy consumption of the system increases due to better comfort conditions guaranteed by the heating system but the intervention of the electric resistance is reduced, since the heat pump operates for a longer period at full load. Moreover, it has been demonstrated that TICL is not effective if the heat pump is coupled to convective emitters as fan-coils: in fact, with convective terminal units, only a reduced quantity of thermal energy is stored within the building envelope and can be released during the coldest part of the day.

In conclusion, TICL could be an effective solution for heating systems based on heat pumps coupled to radiant emitters by generating a significant enhancement of the system seasonal energy performance, improved internal comfort conditions and, at the same time, enabling the adoption of downsized heat pumps, thus reducing installation costs.

Author Contributions: Conceptualization, M.D., P.V. and C.N.; methodology, M.D.; software, M.D. and P.V.; validation, C.N.; formal analysis, C.N.; investigation, M.D., P.V. and C.N.; resources, P.V.; data curation, M.D. and P.V.; writing—original draft preparation, C.N.; writing—review and editing, M.D. and P.V.; visualization, P.V.; supervision, G.L.M.; project administration, G.L.M.; funding acquisition, G.L.M. All authors discussed and provided comments at all stages. All authors have read and agreed to the published version of the manuscript.

Funding: This research was funded by RdS PTR 2019–2021, agreement between Ministry of Economic Development and ENEA (2019–2021), 1st year; Research objective "Electric system", Work package: LA10, LA11, and LA17.

Conflicts of Interest: The authors declare no conflict of interest.

Nomenclature

Abbreviations	
COP	Coefficient of performance
E	Energy (kWh)
K_p	Proportional gain
P	Power (kW)
PMV	Predicted mean vote
SCOP	Seasonal coefficient of performance
$SCOP_{net}$	Net seasonal coefficient of performance
T	Temperature (°C)
T_{biv}	Bivalent temperature (°C)
T_d	Derivative time (s)
T_i	Integral time (s)
TICL	Thermal inertia control logic
φ	Frequency (Hz)
V	Volumetric flow rate ($m^3\ h^{-1}$)
Subscripts	
1	First intermediate frequency
2	Second intermediate frequency
air	Air
el	Electrical
ER	Electric resistance
fan	Fan
FC	Fan-coil
h	Heating
HP	Heat pump
min	Minimum
max	Maximum
out	Outlet
RF	Radiant floor
th	Thermal
tot	Total
w	Water

References

1. European Commission. Energy—Energy Efficiency in Buildings. Available online: https://ec.europa.eu/energy/en/topics/energy-efficiency/buildings (accessed on 30 July 2020).
2. European Commission. Climate Action Paris Agreement. Available online: https://unfccc.int/process-and-meetings/the-paris-agreement/the-paris-agreement (accessed on 30 July 2020).
3. Building Performance Institute Europe (BPIE). Europe's Buildings under the Microscope. Available online: http://bpie.eu/wp-content/uploads/2015/10/HR_EU_B_under_microscope_study.pdf (accessed on 30 July 2020).
4. Ministero dello Sviluppo Economico (MISE). La Situazione Energetica Nazionale nel 2018. Available online: https://www.mise.gov.it/images/stories/documenti/relazione_annuale_situazione_energetica_nazionale_dati_2018.pdf (accessed on 30 July 2020).
5. Loreti, L.; Valdiserri, P.; Garai, M. Dynamic simulation on energy performance of a school. *Energy Procedia* **2016**, *101*, 1026–1033. [CrossRef]
6. Sun, X.; Jovanovic, J.; Zhang, Y.; Fan, S.; Chu, Y.; Mo, Y.; Liao, S. Use of encapsulated phase change materials in lightweight building walls for annual thermal regulation. *Energy* **2019**, *180*, 858–872. [CrossRef]
7. Domínguez, S.; Sendra, J.J.; León, A.L.; Esquivias, P.M. Towards Energy Demand Reduction in Social Housing Buildings: Envelope System Optimization Strategies. *Energies* **2012**, *5*, 2263–2287. [CrossRef]

8. Ascione, F.; Bianco, N.; Mauro, G.M.; Napolitano, D.F. Building envelope design: Multi-objective optimization to minimize energy consumption, global cost and thermal discomfort. Application to different Italian climatic zones. *Energy* **2019**, *174*, 359–374. [CrossRef]
9. Baglivo, C.; Congedo, P.M.; Di Cataldo, M.; Coluccia, L.D.; D'Agostino, D. Envelope design optimization by thermal modelling of a building in a warm climate. *Energies* **2017**, *10*, 1808. [CrossRef]
10. Cesari, S.; Valdiserri, P.; Coccagna, M.; Mazzacane, S. The energy saving potential of wide windows in hospital patient rooms, optimizing the type of glazing and lighting control strategy under different climatic conditions. *Energies* **2020**, *13*, 2116. [CrossRef]
11. Cesari, S.; Valdiserri, P.; Coccagna, M.; Mazzacane, S. Energy savings in hospital patient rooms: The role of windows size and glazing properties. *Energy Procedia* **2018**, *148*, 1151–1158. [CrossRef]
12. European Commission. Directive 2018/844/EU of the European Parliament and of the Council Amending Directive 2010/31/EU on the Energy Performance of Buildings and Directive 2012/27/EU on Energy Efficiency. 2018. Available online: https://eur-lex.europa.eu/legal-content/EN/TXT/HTML/?uri=CELEX:32018L0844&from=EN (accessed on 28 September 2020).
13. Jensen, S.O.; Marszal-Pomianowska, A.; Lollini, R.; Pasut, W.; Knotzer, A.; Engelmann, P. IEA EBC Annex 67 Energy Flexible Buildings. *Energy Build.* **2017**, *155*, 25–34. [CrossRef]
14. Dominkovic, D.F.; Gianniou, P.; Münster, M.; Heller, A.; Rode, C. Utilizing thermal building mass for storage in district heating systems: Combined building level simulations and system level optimization. *Energy* **2018**, *153*, 949–966. [CrossRef]
15. Romanchenko, D.; Nyholm, E.; Odenberger, M.; Johnsson, F. Flexibility potential of space heating demand response in buildings for district heating systems. *Energies* **2019**, *12*, 2874. [CrossRef]
16. Saafi, K.; Daouas, N. Energy and cost efficiency of phase change materials integrated in building envelopes under Tunisia Mediterranean climate. *Energy* **2019**, *187*, 2874. [CrossRef]
17. Marani, A.; Nehdi, M.L. Integrating phase change materials in construction materials: Critical review. *Constr. Build. Mater.* **2019**, *217*, 36–49. [CrossRef]
18. Johra, H.; Heiselberg, P.; Le Dreau, J. Influence of envelope, structural thermal mass and indoor content on the building heating energy flexibility. *Energy Build.* **2019**, *183*, 325–339. [CrossRef]
19. Lu, S.; Liang, R.; Zhang, J.; Zhou, C. Performance improvement of solar photovoltaic/thermal heat pump system in winter by employing vapor injection cycle. *Appl. Therm. Eng.* **2019**, *155*, 135–146. [CrossRef]
20. Sarbu, I.; Sebarchievici, C. Performance evaluation of radiator and radiant floor heating systems for an office room connected to a ground-coupled heat pump. *Energies* **2016**, *9*, 228. [CrossRef]
21. Lucchi, M.; Lorenzini, M.; Valdiserri, P. Energy performance of a ventilation system for a block of apartments with a ground source heat pump as generation system. *J. Phys. Conf. Ser.* **2017**, *796*, 12034. [CrossRef]
22. Arteconi, A.; Hewitt, N.J.; Polonara, F. Domestic demand-side management (DSM): Role of heat pumps and thermal energy storage (TES) systems. *Appl. Therm. Eng.* **2013**, *51*, 155–165. [CrossRef]
23. Liu, M.; Heiselberg, P. Energy flexibility of a nearly zero-energy building with weather predictive control on a convective building energy system and evaluated with different metrics. *Appl. Energy* **2019**, *233*, 764–775. [CrossRef]
24. Klein, S.A.; Duffie, A.J.; Mitchell, J.C.; Kummer, J.P.; Thornton, J.W.; Bradley, D.E.; Arias, D.A.; Beckman, W.A.; Duffie, N.A.; Braun, J.E.; et al. *TRNSYS 17: A Transient System Simulation Program*; University of Wisconsin: Madison, WI, USA, 2010.
25. Klein, S.A.; Duffie, A.J.; Mitchell, J.C.; Kummer, J.P.; Thornton, J.W.; Bradley, D.E.; Arias, D.A.; Beckman, W.A.; Duffie, N.A.; Braun, J.E.; et al. *TRNSYS 17—A TRaNsient SYstem Simulation Program, User Manual. Multizone Building Modeling with Type 56 and TRNBuild. Version 17.1*; University of Wisconsin: Madison, WI, USA, 2012; Volume 5.
26. Dott, R.; Haller, M.; Ruschenburg, J.; Ochs, F.; Bony, J. IEA-SHC Task 44 Subtask C Technical Report: The Reference Framework for System Simulations of the IEA SHC Task 44/HPP Annex 38: Part B: Buildings and Space Heat Load. IEA-SHC. 2013. Available online: http://www.taskx.iea-shc.org/data/sites/1/publications/T44A38_Rep_C1_B_ReferenceBuildingDescription_Final_Revised_130906.pdf (accessed on 28 September 2020).

27. EN ISO 7730. Ergonomics of the Thermal Environment—Analytical Determination of Thermal Comfort by Using Calculation of the PMV and PPD Indices and Local Thermal Comfort Criteria. 2005. Available online: https://standards.cen.eu/dyn/www/f?p=204:110:0::::FSP_PROJECT,FSP_ORG_ID:3603,6104&cs=174E4319C250BD68D73B1BF5E1B13A151 (accessed on 28 September 2020).
28. EN 1264. Water Based Surface Embedded Heating and Cooling Systems. 2007. Available online: https://standards.cen.eu/dyn/www/f?p=204:32:0::::FSP_ORG_ID,FSP_LANG_ID:6112,25&cs=1FB43CF4AA26832B0882A93C1B983130F (accessed on 28 September 2020).
29. EN 14825. Air Conditioners, Liquid Chilling Packages and Heat Pumps, with Electrically Driven Compressors, for Space Heating and Cooling—Testing and Rating at Part Load Conditions and Calculation of Seasonal Performance. 2016. Available online: https://www.en-standard.eu/din-en-14825-air-conditioners-liquid-chilling-packages-and-heat-pumps-with-electrically-driven-compressors-for-space-heating-and-cooling-testing-and-rating-at-part-load-conditions-and-calculation-of-seasonal-performance/ (accessed on 28 September 2020).